Interfacial Engineering of Montmorillonite Clay in Electrospun PVdF-co-HFP Nanocomposite Separator for High-Performance Sodium Ion Battery

Akash Kankane[1], Dhirendra Kumar Rai[2], S K Srivastava[3], S Janakiraman[1]

[1]Department of Mechanical Engineering, Indian Institute of Technology Indore, INDIA

[2]Department of Metallurgical Engineering and Materials Science, Indian Institute of Technology Indore, INDIA

[3]Department of Physics, Bundelkhand University, Jhansi, India

In electrospinning, the rheological behavior of the precursor solution plays a crucial role in determining the resultant fiber morphology. As the MMT content increased from 0 to 10 wt% in the PVdF-co-HFP/DMSO system, a progressive rise in solution viscosity was observed, which directly influenced the fiber-forming dynamics. At high filler loading (10 wt%), the viscosity reached ~2600 mPa.s, leading to limited jet stretching and the formation of thick fibers. In contrast, the formulation containing 5 wt% MMT exhibited an optimal viscosity of ~2280 mPa.s, enabling stable jet formation and sufficient elongation during electrospinning. This produced a uniform nanofiber with an average diameter of ~300 nm, resulting in a well-interconnected nanoscale pore structure. The finer fiber diameter at 5 wt% enhances electrolyte uptake, ionic conductivity, and interfacial contact while maintaining mechanical integrity.

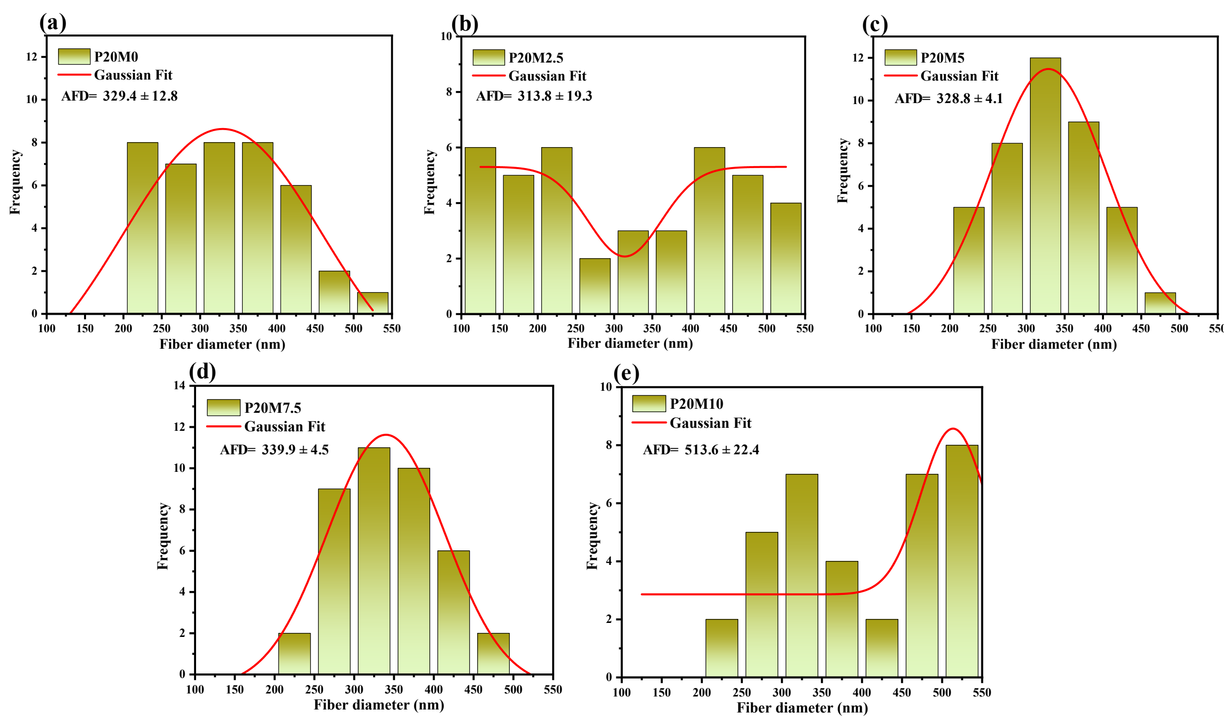

Fig. S1 Histogram of fiber diameter distribution for (a) P20M0, (b) P20M2.5, (c) P20M5, (d) P20M7.5, (e) P20M10.

Table S1: Viscosity values of the solutions measured by a rotational viscometer.

Solution (PVdF-co-HFP in DMSO solvent)	Viscosity (mPa.s)
0 % MMT	2050±5
2.5 % MMT	2140±10
5 % MMT	2280±5
7.5 % MMT	2410±10
10 % MMT	2590±10

Table S2 Ionic conductivity of PP, electrospun pristine and nanocomposite separators.

Materials	Thickness (µm)	Bulk resistance (Ω)	Ionic Conductivity, σ (mS cm^{-1})
PP	25	5.19	0.24
P20	60	3.04	0.98
P20M2.5	64	2.17	1.47
P20M5	70	1.88	1.85
P20M7.5	75	2.30	1.62
P20M10	80	2.91	1.37

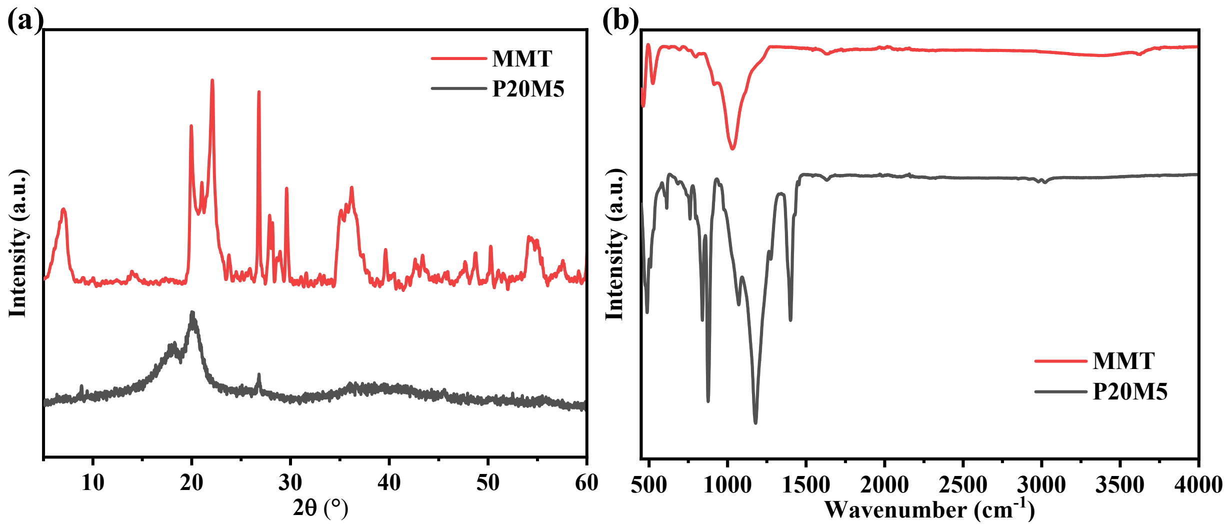

Fig. S2 (a) XRD and (b) FTIR plots for MMT powder and electrospun nanocomposite separator P20M5.

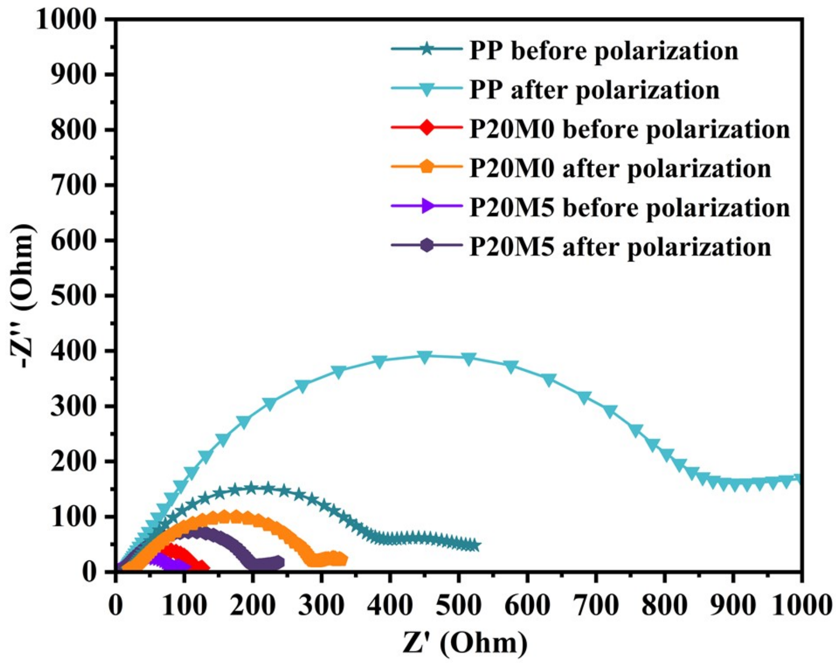

Fig. S3 Nyquist plot of various Na/SES/Na systems before and after polarization, at room temperature.

Table S3 Specific charge and discharge capacity of fabricated separators in NFM111/SES/Na half-cell at 0.1 C-rate.

Separators	Specific charge capacity (mA h g^{-1})	Specific discharge capacity (mA h g^{-1})	β-Phase (%)
P20M0	160.45	160.40	61
P20M2.5	165.50	163.98	58
P20M5	167.30	166.71	63
P20M7.5	156.01	155.08	60
P20M10	150.15	150.03	54

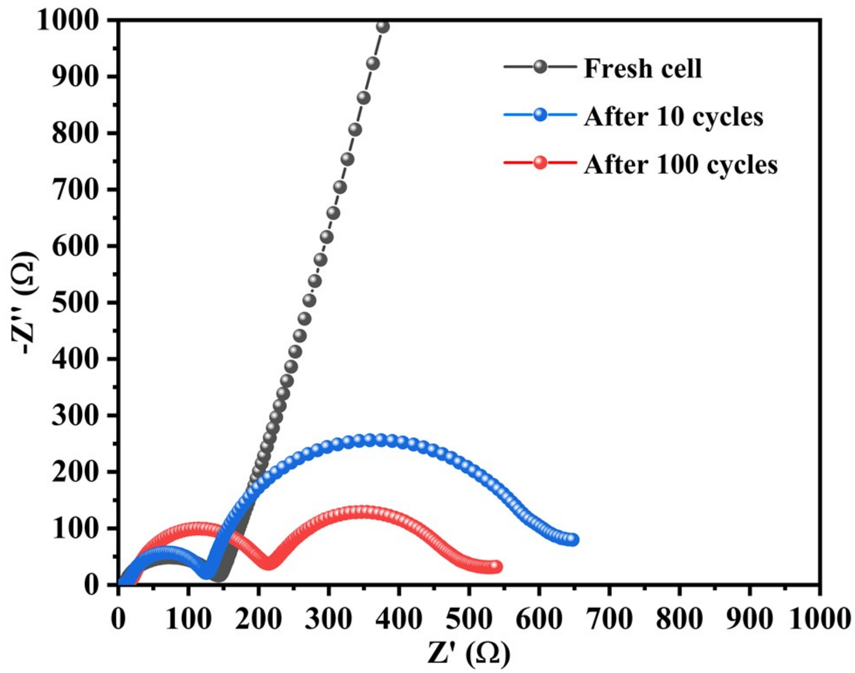

Fig. S4 EIS spectra of the assembled half-cell fabricated with P20M5 separator before and after cyclic stability test.

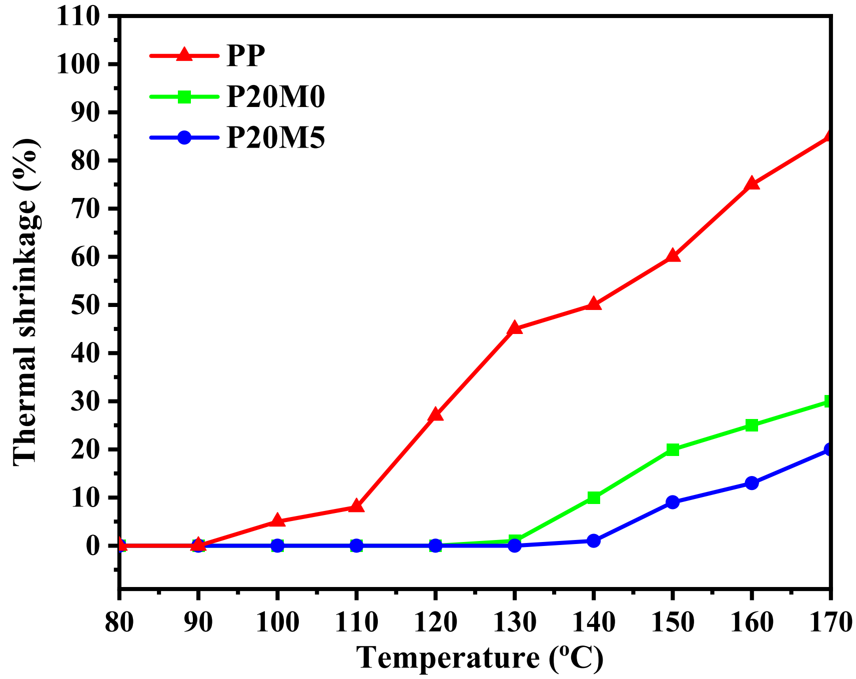

Fig. S5 Thermal shrinkage ratios for PP, P20M0, and P20M5 membranes at different temperatures.

Table S4. Comparison of the present work with previously reported electrospun separators for SIBs.

Electrospun separator	**Electrolyte**	**Ionic conductivity (mS cm^{-1})**	**Electrochemical stability (V) vs Na^+/Na**	**References**
PAN	1 M $NaPF_6$, EC: DMC, (1:1 v/v)	1.70	4.06	1
PAN/Al_2O_3/cellulose	1 M $NaPF_6$, EC: DEC, (1:1 v/v)	0.49	4.50	2
PVDF	1 M $NaPF_6$, EC: PC,	1.08	5.0	3

	(1:1 v/v)			
PVDF	1 M $NaClO_4$, in EC: DEC, (1:1 v/v)	0.92	5.0	4
PVDF/PP	1 M $NaClO_4$, in EC: DEC, (1:1 v/v)	1.25	4.80	5
PVDF-Al_2O_3/PE	1 M $NaPF_6$, PC: EMC: DEC, (1:1:1 v/v/v)	0.35	4.65	6
PVDF-HFP	1 M $NaClO_4$, EC:DEC, (1:1 v/v)	1.13	4.80	7
PVDF-HFP/PAN	1 M $NaClO_4$, EC:PC, (1:1 v/v)	1.40	4.90	8
PVDF-co-HFP/MMT	1 M $NaClO_4$, EC:PC, (1:1 v/v)	1.85	4.90	**This work**

References

1 X. Guo, X. Li, Y. Xu, J. Chen, M. Lv, M. Yang and W. Chen, *J. Phys. Chem. C*, 2022, **126**, 8238–8247.

2 L. Zhou, Z. Hou, X. Kong, S. Pan, B. Liu, T. Zhao, X. Jiang, Z. Shi and J. Wang, *Journal of Power Sources*, 2026, **662**, 238792.

3 S. Janakiraman, A. Surendran, R. Biswal, S. Ghosh, S. Anandhan and A. Venimadhav, *Mater. Res. Express*, 2019, **6**, 086318.

4 S. Janakiraman, A. Surendran, R. Biswal, S. Ghosh, S. Anandhan and A. Venimadhav, *Journal of Electroanalytical Chemistry*, 2019, **833**, 411–417.

5 S. Janakiraman, M. Khalifa, R. Biswal, S. Ghosh, S. Anandhan and A. Venimadhav, *Journal of Power Sources*, 2020, **460**, 228060.

6 B. Li, Y. Liu, X. Han, Y. Zhou, F. Xiao, W. Xian, Y. Chu, G. Liu and Z. Lu, *Chemical Engineering Journal*, 2024, **501**, 157803.

7 S. Janakiraman, O. Padmaraj, S. Ghosh and A. Venimadhav, *Journal of Electroanalytical Chemistry*, 2018, **826**, 142–149.

8 A. Kankane, D. K. Rai and S. Janakiraman, *ACS Appl. Nano Mater.*, 2025, **8**, 18740–18750.